LAWRENCE
LIVERMORE
NATIONAL
LABORATORY

LLNL-JRNL-471625

Temperature and vital effect controls on Bamboo coral (Isididae) isotopegeochemistry: A test of the ¿lines method¿

T. M. Hill, H. J. Spero, T. P. Guilderson, M. LaVigne, D. Clague, S. Macalello, N. Jang

March 2, 2011

Geochemistry, Geophysics, Geosystems

Disclaimer

Temperature and vital effect controls on Bamboo coral (*Isididae*) isotope geochemistry: A test of the "lines method"

Hill, T.M.[a,b], Spero, H.J.[a], Guilderson, T.[c,d], LaVigne, M.[a,b], Clague, D.[e], Macalello, S.[b], Jang, N.[b]

Running title: Bamboo coral isotope geochemistry

[a] Department of Geology, University of California, Davis, CA 95616 USA
[b] Bodega Marine Laboratory, University of California, Davis
[c] Center for Accelerator Mass Spectrometry, Lawrence Livermore National Laboratory P.O. Box 808, L-397, Livermore CA 94550 USA
[d] Institute of Marine Sciences, University of California, Santa Cruz, CA 95064 USA
[e] Monterey Bay Aquarium Research Institute, 770 Sandholdt Road, Moss Landing, CA 95039

ABSTRACT

Deep-sea bamboo corals hold promise as long-term climatic archives, yet little information exists linking bamboo coral geochemistry to measured environmental parameters. This study focuses on a suite of ten bamboo corals collected from the Pacific and Atlantic basins (250-2136 m water depth) to investigate coral longevity, growth rates, and isotopic signatures. Calcite samples for stable isotopes and radiocarbon were collected from the base the corals, where the entire history of growth is recorded. In three of the coral specimens, samples were also taken from an upper branch for comparison. Radiocarbon and growth band width analyses indicate that the skeletal calcite precipitates from ambient dissolved inorganic carbon (DIC) and that the corals live for 150-300 years, with extension rates of 9-128 microns/year. A linear relationship between coral calcite $\delta^{18}O$ and $\delta^{13}C$, indicates that the isotopic composition is influenced by vital effects ($\delta^{18}O$:$\delta^{13}C$ slope of 0.17-0.47). As with scleractinian deep-sea corals, the intercept from a linear regression of $\delta^{18}O$ vs. $\delta^{13}C$ is a function of temperature, such that a reliable paleotemperature proxy can be obtained, using the "lines method" [*Smith et al.,* 2000; *Adkins et al.*, 2003]. Although the coral calcite $\delta^{18}O$:$\delta^{13}C$ slope is maintained throughout the coral base ontogeny, the branches and central cores of the bases exhibit $\delta^{18}O$:$\delta^{13}C$ values that are shifted far from equilibrium. We find that a reliable intercept value can be derived from the $\delta^{18}O$:$\delta^{13}C$ regression of multiple samples distributed throughout one specimen, or multiple samples within individual growth bands.

1. INTRODUCTION

Studies have shown that deep-sea corals (DSC) are important archives for reconstructing past ocean circulation and environmental variability [e.g., *Smith et al*., 2000; *Adkins et al.,* 2003; *Thresher et al.,* 2004; *Robinson et al*., 2005; *Roark et al.,* 2005; *Sherwood et al.,* 2005; *Tracey et al*., 2007; *Sherwood et al.,* 2008; *Sherwood and Edinger,* 2009; *Thresher et al.,* 2009]. However, these records are not without complications when interpreting stable isotopic data with respect to equilibrium conditions at the time the corals were alive. Previous studies have focused primarily on interpreting the offset from isotopic equilibrium observed in shallow and deep-water aragonitic coral skeletons [e.g., *Emiliani et al*., 1978; *Heikoop et al*., 2000*; Smith et al.,* 2000*; Adkins, et al.,* 2003*; Sinclair et al.,* 2006]. One study of the aragonitic deep-sea coral *Desmophyllium cristagalli* showed that randomly selected samples of single coral specimens exhibit a wide range of $\delta^{18}O$ and $\delta^{13}C$ values and that some regions of the coral approach isotopic equilibrium whereas others do not [*Smith et al.,* 2000].

Smith et al. [2000] reported that multiple isotopic analyses of 35 coral specimens (18 species) displayed a linear trend between skeletal $\delta^{18}O$ and $\delta^{13}C$ with slopes ranging between 0.23-0.67. The most positive $\delta^{18}O$ values approached isotopic equilibrium for ambient conditions, and the y-intercept of the $\delta^{18}O$ and $\delta^{13}C$ regression can, in principle, could be used for paleotemperature reconstructions ("lines method"; [*Smith et al.,* 2000]). Further investigation of *D. cristagalli* using microsampling techniques indicated that regions of rapid growth were further from isotopic equilibrium (more depleted in ^{18}O and ^{13}C) than those regions associated with slowly accumulating, less dense aragonite [*Adkins*

63 *et al.,* 2003]. Currently, data comparing vital effects and growth structures have been
64 largely limited to *D. cristagalli*. Additional data from other deep-sea coral taxa and
65 mineralogies (e.g., calcitic corals) are needed to determine whether DSC skeletal $\delta^{18}O$
66 and $\delta^{13}C$ data can be more broadly used to compute temperatures for paleoceanographic
67 applications [e.g., *Druffel et al.,* 1995; *Heikoop et al.,* 2002].
68
69 Here we present the first systematic investigation of the carbon and oxygen isotope
70 content of a suite of radiometrically-dated deep-sea bamboo corals (family *Isididae*;
71 Table 1). Bamboo corals colonize intermediate to deep-water depths (400 to >3000m) in
72 most ocean basins and are long lived (>100 years). Some specimens clearly show distinct
73 annual banding and sub-annual trace elemental cycles [*Roark et al., 2005*; *Andrews et al.,*
74 2009; *Thresher et al*., 2009]. Bamboo corals precipitate a skeleton composed of both
75 calcite internodes and organic nodes (Fig. 1). The flux of organic carbon from surface
76 waters serves as the primary food source for these organisms, and contributes to the
77 geochemistry of the organic nodes [*Roark et al.,* 2005; *Myrvold et al.,* 2007]. Previous
78 research has shown that gorgonin in bamboo corals is used to construct the nodes as well
79 as distribute seams of organic material throughout the calcite skeleton, presumably to
80 give the skeletal framework flexibility [*Noé and Dullo*, 2006]. The calcite skeleton is
81 composed of high-Mg calcite precipitated from surrounding seawater dissolved inorganic
82 carbon (DIC; 7-10 mol% $MgCO_3$; [*Roark et al.,* 2005; *Noé and Dullo*, 2006]). By
83 calibrating the "lines method" in modern corals, this study provides the first evidence that
84 bamboo coral isotope geochemistry can be used as an archive of intermediate water
85 temperature.

2. METHODS

This study focuses on 10 corals collected via submersible, dredge or trawl from the California margin, Gulf of Alaska, Florida Straits, and Bowditch Seamount, near Bermuda (Table 1; Figure 2). With the exception of the Bowditch Seamount coral (BE 1) and the Bodega, CA coral (BB), all specimens were observed to have living polyps on their skeleton at the time of collection. Bamboo coral (*Isididae*) taxonomic identification is currently undergoing revision, so multiple related species may be represented in the data presented here.

The bamboo corals were sectioned to yield calcite disks for thin sections, photography and geochemical analyses. Disks were cut from the base or bottom of a branch, to avoid any embedded branches within the section. Thin sections were polished to 100-200 μm thickness. The corals were sampled for isotope and radiocarbon analyses using a drill press (500 μm diameter bit), a Merchantek microsampler, or a dremel drill, depending on the desired sample size. Coral sections were sampled perpendicular to the radial growth axis from margin to center. Samples were acquired every 1 mm, with the exception of BB which was micromilled every 0.25 mm. Additional samples were acquired from coral BB from within a single growth band 10 mm from the margin (sampled parallel to growth axis; 24 samples, 2-4 mm sampling distance).

Photomicrographs were taken of four of the California margin specimens using a Fisher digital inverted microscope and Micron software package that enables the measurement of individual growth bands (repeated measurement of the same tracks yield error of +/-

111 10 μm). To compare growth band width to radiocarbon-derived growth rates for a
112 selection of the California margin corals, the width of bands identified by dark/light pairs
113 within the calcite were measured for each coral thin section to determine a radial
114 extension rate for that section (Table 2). The bands were measured from the outer 1 mm
115 of the coral (5-25 bands per coral); the average, standard error and standard deviation (1
116 sigma) of the widths were calculated for these measurements (Table 2). For this analysis,
117 all banding features were assumed to reflect one year of growth. Radial extension rates
118 wer calculated from these measurements utilizing the one sigma standard deviation for
119 each coral (Table 3).
120
121 Water samples corresponding to four of the California Margin corals were collected with
122 Niskin bottles aboard the *ROV Tiburon* from locations near the coral collection sites
123 (1842-2136m) for the purpose of radiocarbon analyses. For radiocarbon analyses, calcite
124 powders and water samples were reacted with 85% orthophosphoric acid (H_3PO_4) *in*
125 *vacuo* and the resulting CO_2 was collected, cryogenically purified and reduced to graphite
126 prior to being analyzed at the Lawrence Livermore National Laboratory Center for
127 Accelerator Mass Spectrometry (CAMS). Results include a background correction based
128 on ^{14}C-free calcite, and $\delta^{13}C$ normalization. Results are reported as conventional
129 (uncorrected) radiocarbon age and per mil (‰) $D^{14}C$ as per international convention put
130 forth in *Stuiver and Polach* [1977], where
131
132 $$D^{14}C = [((^{14}C/^{12}C_{sample})/(^{14}C/^{12}C_{1950}))-1] \times 1000 \quad \text{(Eq. 1)}$$

133 These $D^{14}C$ measurements were utilized to compare the $D^{14}C$ content of coral calcite and
134 seawater DIC. Derived radiocarbon ages (uncalibrated) were then used to calculate
135 average radial extension rates for each coral ($\mu m/^{14}C$ years; Table 3). Coral extension
136 rates are calculated using the minimum and maximum radiocarbon age from two
137 locations on the coral thin section (e.g., 0-1 mm and 11-12 mm).
138
139 Stable isotope analyses for all corals except ALV3808-3 were conducted on sample
140 powders using a Fisons Optima isotope ratio mass spectrometer (IRMS) at UC Davis.
141 Roasting and other cleaning steps were avoided because preliminary analyses suggested
142 these procedures alter the isotopic values of coral calcite. The calcite powders were
143 reacted *in vacuo* with 105% orthophosphoric acid at 90°C using an ISOCARB automated
144 common acid bath system. For sample ALV3808-3 (Warwick Seamount), samples were
145 analyzed at the Stanford Stable Isotope Laboratory on a Finnigan MAT 252 IRMS after
146 being reacted at 70°C in a Kiel-III device. Instrument precision for calcite $\delta^{18}O$ and $\delta^{13}C$
147 was ±0.06‰ (±1σ) in both laboratories, based on multiple analyses of laboratory calcite
148 standards.
149
150 We correct for offsets between corals due to local $\delta^{18}O_{water}$ and $\delta^{13}C_{DIC}$ by subtracting
151 isotopic values measured from seawater samples for each coral. For California corals, a
152 water sample was acquired near coral T664 A1 (1295m) at the time of coral sampling and
153 analyzed at UC Davis. Water $\delta^{18}O$ was determined via CO_2 equilibration using an
154 automated equilibrator attached to a Finnigan MAT 251 IRMS at UC Davis. The
155 precision of $\delta 18O_w$ replicates was ± 0.03‰ (± 1 σ). For $\delta^{13}C_{DIC}$, CO_2 was evolved from

156 seawater on a vacuum extraction line and analyzed using a Fisons Optima IRMS. For
157 Bowditch Seamount, Florida Straights and Gulf of Alaska corals, previously published
158 $\delta^{18}O_w$ and $\delta^{13}C_{DIC}$ data are utilized [*Epstein and Mayeda*, 1953; *Ostlund and Grall*, 1987;
159 *Schmidt et al.,* 1999; *Guilderson et al*., 2002].
160
161 All calcite oxygen and carbon isotope data and $\delta^{13}C_{DIC}$ data are presented relative to the
162 Vienna Pee Dee Belemnite (V-PDB) standard; water oxygen isotope data are presented
163 relative to Vienna Standard Mean Ocean Water (V-SMOW) standard. Data are presented
164 in standard per mil (‰) notation where:

165 $$\delta^{18}O\ (^{13}C) = [((^{18}O/^{16}O_{sample})/(^{18}O/^{16}O_{standard})) -1] \text{ X } 1000 \quad \text{(Eq. 2)}$$

166

167 **3. RESULTS**

168 Coral growth rates calculated from growth-band measurements ranged from 14-126
169 μm/year (Table 2). These extension rates estimates do not reveal a consistent pattern of
170 the coral base growing faster than the branch or vice versa (average base extension rates:
171 21-77 μm/year; mean branch extension rates: 14-126 μm/year; Table 2).
172
173 Radiocarbon analyses of several California margin corals yield a calcite $D^{14}C$ range of
174 -220 to -289‰ (+/-2-6‰; Table 3). Seawater DIC values from nearby collection sites
175 yield ambient $D^{14}C$ values between -229.4 to -268.9‰ (+/- 2.1-4.0‰).
176
177 Radial extension rates were calculated from the $D^{14}C$ measurements, for comparison to
178 radial extension rates calculated from the band width measurements (Table 3). In four of

179 the five corals, the radial extension rate estimates overlap using radiocarbon and band
180 width methods, but there is not complete agreement between these methods and the
181 estimated ranges are very large.
182
183 Oxygen and carbon isotope data from the corals range between 0 to 2.7‰, and -5.5 to
184 2‰, respectively (Table 4). A complete transect of $\delta^{18}O$ and $\delta^{13}C$ values from margin to
185 core is shown for one coral (BB), along with a corresponding micrograph indicating
186 sample locations (Fig. 3). This coral exhibits a range of $\delta^{18}O$ and $\delta^{13}C$ values ($\delta^{18}O$ = 0.2
187 to 1.4‰; $\delta^{13}C$ = -1.5 to -4.4‰), including decreased $\delta^{18}O$ and $\delta^{13}C$ values towards the
188 central core of the sample. In the remaining figures and calculations, samples very near
189 the central core of the corals were avoided, because of anomalous $\delta^{13}C$ and $\delta^{18}O$ values
190 commonly observed there (values more than 1‰ depleted relative to nearby samples
191 were excluded).
192
193 In the remaining results, corals are corrected for local $\delta^{18}O_w$ and $\delta^{13}C_{DIC}$ unless otherwise
194 specified. For California corals we utilized a water sample acquired near coral T664 A1
195 (33.13°N, 120.91°W, 1295m): $\delta^{18}O_w$ = -0.13‰, $\delta^{13}C_{DIC}$ =0.08‰. For Bowditch
196 Seamount and Florida Straights corals, previously published $\delta^{18}O_w$ data are utilized:
197 $\delta^{18}O_w$ = 0.34‰ (from 28.08°N 60.82°W, 2000m [*Epstein and Mayeda*, 1953; *Schmidt et*
198 *al.,* 1999]) and $\delta^{13}C_{DIC}$ =0.70 (from 28.21°N -53.79°W, 1981m [*Ostlund and Grall*,
199 1987]). For Gulf of Alaska (ALV3803) coral, published data from nearby sites was
200 utilized ($\delta^{18}O_w$ = -0.20‰, $\delta^{13}C_{DIC}$ = -0.71‰ [*Guilderson et al*., 2002]).
201

202 We observe a $\delta^{18}O$:$\delta^{13}C$ relationship from data collected across the basal (thickest) part
203 of the corals, with a slope between 0.17-0.47 (Fig. 4; Table 4-6). The linear regressions
204 of $\delta^{18}O$:$\delta^{13}C$ are statistically significant in 9 of the 10 specimens analyzed ($p<0.1$; Table
205 5; FL-17-XI-05-1-11 was not significant). Stable isotope data from branch and base
206 samples are plotted for 3 of the corals (Fig. 5). Although the same slope is observed as
207 previously noted (0.37 for the whole dataset of base/branch samples), branch samples are
208 1-2‰ more depleted in ^{18}O and ^{13}C than base samples (Fig. 5). Based upon the
209 measurements of growth bands listed in Table 2, there is no statistical relationship
210 between coral growth rate and slope or intercept of the $\delta^{18}O$:$\delta^{13}C$ regression (for slope
211 n=6, R^2= 0.16, for intercept n=6, R^2= 0.41).
212
213 To understand the relationship between the $\delta^{18}O$:$\delta^{13}C$ regression and temperature, we
214 follow the procedure of *Smith et al.* [2000] in making use of a $\delta^{18}O$ vs. $\delta^{13}C$ linear
215 regression line ($\delta^{18}O = m * \delta^{13}C + b$ where *m* is the slope and *b* is the intercept when
216 $\delta^{13}C=0$) for each individual coral (bases only, not branches) as a potential method to
217 reconstruct temperature at the time of skeletal formation ("lines method"; Table 4; Figure
218 6). Two corals were excluded from this analysis: the FL-17-XI-05-1-11 specimen that did
219 not yield a statistically significant $\delta^{18}O$:$\delta^{13}C$ regression line, and the BB (Bodega) coral
220 which was sampled by fishing trawl and the sampling depth (and therefore temperature)
221 are approximate (Table 5). The temperature regression yields a linear relationship with
222 R^2= 0.92 ($p < 0.001$). Because the ultimate intention of this study is to enable prediction
223 of paleotemperatures in fossil bamboo coral specimens, temperature is plotted on the y-
224 axis and 95% confidence intervals are provided (Fig. 6).

225

226 A set of 24 samples drilled within an individual growth band in the BB coral yield a total
227 $\delta^{18}O$ range of 1.12 to 1.76‰, and $\delta^{13}C$ range of -1.58 to -4.57‰ prior to correction for
228 $\delta^{18}O_w$ and $\delta^{13}C_{DIC}$. These data indicate that skeletal heterogeneity exists within samples
229 that were presumably precipitated within one year; this type of analysis would be
230 necessary for the "lines method" to be used in time series (Fig.7). The $\delta^{18}O$:$\delta^{13}C$
231 regression from coral BB data yields a linear relationship with an intercept of 2.10‰ and
232 a slope of 0.21 ($R^2 = 0.74$, $p < 0.001$; Fig. 7).

233

234 **4. DISCUSSION**

235 **4.1 Radiocarbon, radial extension rate and coral lifespan**

236 $D^{14}C$ of samples taken from outer margin (within 1 mm) agree well with the ambient
237 water $D^{14}C_{DIC}$ collected from the same depths, with outer margin samples ranging
238 between -220.3 to -276.7‰, and water samples range from -229.4 to -268.9‰ (Table 3).
239 These $D^{14}C$ values indicate that the corals are precipitating calcite from ambient
240 seawater, with radiocarbon ages between 2000-2500 years before present (YBP).
241 Bowditch Seamount coral, BE-1, yielded a radiocarbon age of 570 years ($D^{14}C$ = -74.8
242 +/- 3.8 ‰; Table 3). This $D^{14}C$ value is consistent with pre-bomb NADW values (-65‰;
243 [*Broecker and Olsson,* 1961]) with a small fraction of older AAIW mixed in. These data
244 support previous observations that deep sea coral $D^{14}C$ values can be used to establish
245 coral age as well as track intermediate water ventilation and/or circulation changes [e.g.,
246 *Druffel et al*., 1995; *Heikoop et al*., 2002; *Roark et al.,* 2005; *Eltgroth et al.,* 2006;
247 *Sherwood et al.,* 2008; *Sikes et al.,* 2008].

This investigation utilizes both band width measurements and radiocarbon analyses to develop an understanding of average coral growth rates. Previous investigations of bamboo coral growth report radial extension rates of <100 to exceeding 500 μm/year [*Andrews et al.,* 2005; *Roark et al.,* 2005; *Noé and Dullo,* 2006; *Noé et al.,* 2008]. Based upon the range of microscopically measured skeletal radial extension rates, specimens in the present study contain average growth rates of 21-77 μm/year for base and 14-126 μm/year for branch cross sections (Table 2). Radial extension rates calculated by this method are extremely variable (standard deviations are large); however, extension rates calculated from radiocarbon analyses overlap with those from annual band width measurements in 4 of the 5 of the corals (Table 3). The lack of complete agreement between these methods may be due to changes in radial extension rate over time; the radiocarbon measurements average over the entire coral (outer edge to center), and the band width measurements focused on only the outer 1 mm. Additionally, radiocarbon measurements on carbonate internodes (reflecting intermediate water masses) may be too approximate to clarify the temporal phasing of skeletal banding features except for when the coral is exceptionally long-lived. Radial extension rates would clearly be improved by increasing the number of bands measured in addition to utilizing other methods for developing independent chronologies (i.e., ^{210}Pb; [*Andrews et al.,* 2009]).

These results indicate that bamboo corals may live for over 300 years, consistent with or longer than existing age estimates on bamboo corals and other deep sea gorgonians [e.g., *Roark et al.*, 2005; *Tracey et al.,* 2007; *Sherwood et al*., 2008; *Sherwood and Edinger,*

2009; *Andrews et al.,* 2009; *Thresher et al.,* 2009]. Base and branch samples indicate these regions of the coral do not record different radial extension rates (Table 2), as discussed further below.

4.2 Oxygen and carbon isotopic values

Oxygen and carbon isotopic values in bamboo corals are clearly impacted by biological processes, or "vital effects", as indicated by strong $\delta^{18}O$:$\delta^{13}C$ relationships. The slopes of the linear regressions of $\delta^{18}O$ vs. $\delta^{13}C$ observed here (0.17-0.47) are similar to the slopes observed previously in aragonitic scleractinian deep-sea corals (0.23-0.67; [*Smith et al.,* 2000]. *Smith et al.* [2000] documented that in the linear $\delta^{18}O$:$\delta^{13}C$ relationship, the most positive $\delta^{18}O$ values approached isotopic equilibrium for ambient conditions. *Smith et al.* [2000] then show that the $\delta^{18}O$ value at the intercept of the regression where $\delta^{13}C=0$ can be used to reconstruct temperature. Thus, a cluster of $\delta^{18}O/\delta^{13}C$ points from an individual coral can produce a regression line that could then be used to determine temperature in fossil corals. Similarly, we have plotted the intercept value where $\delta^{13}C=0$ for each of the corals studied here against temperature (base samples only), corrected for local $\delta^{18}O_w$ and $\delta^{13}{}_{DIC}$ values as described above (Fig. 6). The bamboo coral data in Figure 6 define a line with the equation (Model I Regression):

$$T=-2.09*\delta^{18}O_{c\text{-}w}+8.25 \qquad (R^2 = 0.92;\ p < 0.001) \qquad \text{(Eqn. 3)}$$

or,

$$\delta^{18}O_{c\text{-}w} = -0.44*T + 3.82‰ \qquad \text{(Eqn. 4)}$$

The 95% confidence interval on the paleotemperature estimate is +/- 0.4°C at the mean

294 $\delta^{18}O$ value (2.33‰) and increases to +/- 0.6°C at the extremes of the dataset (Figure 6).
295 As in *Smith et al.* [2000], our primary goal was to establish a predictive relationship for
296 temperature based on $\delta^{18}O$ intercept values. Model I regression provides the simplest
297 analytical framework under these circumstances, and is the preferred approach. In other
298 cases, however (for example, if one desires to understand an underlying mechanistic or
299 functional relationship between variables), Model II regression methods may be required.
300 A Model II regression is characterized by a slope that equals the geometric mean of the
301 slopes of the linear regression of Y on X, and X on Y; this analysis can be used if there is
302 error in both X and Y. Model I and Model II are linked mathematically, by the simple
303 relationship that the slope of the Model II is equal to the slope of Model I divided by R.
304 Therefore, when the R^2 values are high, there is little difference between the slopes using
305 these two models. Using Model II, the slope of the regression line though our data would
306 decline slightly, to -2.17. Confidence intervals for a given $\delta^{18}O$ intercept would remain
307 the same.
308
309 The relationship between $\delta^{18}O$ and temperature in our study exhibits a different intercept
310 and slope compared to *Smith et al*. [2000] such that the lines do not overlap. The different
311 intercept-temperature relationships between these two studies may be due to differences
312 in mineralogy (calcite vs. aragonite).
313
314 When isotopic data from coral branches are considered (using 3 of the California corals),
315 a similar $\delta^{18}O$:$\delta^{13}C$ slope is observed relative to the base samples (0.37). However, there
316 appears to be a stronger offset from equilibrium (ambient seawater) in the branch samples

317 (Fig. 5). A similar pattern is observed when considering isotopic shifts across the
318 structure of the base of a coral (Fig. 3). Based on one of the corals studied here (BB), the
319 $\delta^{13}C$ and $\delta^{18}O$ values show little variability when sampled perpendicular to growth axis,
320 (in contrast to results from within one growth band; Fig. 7), except for the last few mm
321 nearest the central core. Here, $\delta^{13}C$ and $\delta^{18}O$ values become more depleted, similar to
322 values exhibited by branch samples.
323
324 In previous studies of *D. cristagalli*, it was shown that regions of rapid growth are further
325 from isotopic equilibrium than those regions associated with slowly accumulating, less
326 dense carbonate [*Adkins et al.,* 2003]. However, based upon growth band measurements
327 and micrograph examinations, the relationship between growth rate and isotopic
328 equilibrium is not straightforward here. Contrary to the previously proposed relationship
329 between growth rate and isotopic fractionation in other corals, branch sections do not
330 have greater radial extension rates than base sections, and there appears to be no
331 relationship between extension rates and regression line slope or intercept.
332
333 Data from coral BB (Fig. 7) provide insight into the variability of calcite $\delta^{18}O$ and $\delta^{13}C$
334 during approximately 1 year, rather than over the lifetime of the coral (as exhibited in
335 other figures). These analyses indicate a similar range in $\delta^{18}O$ and $\delta^{13}C$ as previously
336 observed in Fig. 4. The regression of $\delta^{18}O$:$\delta^{13}C$ yields a linear relationship with an
337 intercept of 2.10‰ (these data were not included in other figures or calculations). This is
338 very similar to the intercept generated by analyses acquired during perpendicular
339 sampling relative to the growth axis from this coral (1.81‰), indicating that a reliable

intercept value (temperature proxy) can be acquired by sampling within individual growth bands rather than averaging over the entire coral. These results suggest that it may be possible to extract a time series of annually integrated coral temperatures from high-resolution sampling of multiple growth bands.

5. CONCLUSIONS

Radiocarbon and growth band measurements indicate that bamboo corals are long lived, ranging from 150-350 years. Bamboo corals indicate a strong relationship between $\delta^{18}O$ and $\delta^{13}C$, similar to aragonitic deep-sea corals and indicative of strong vital effects influencing the stable isotopic composition (slopes of $\delta^{18}O$:$\delta^{13}C$ regression range from 0.17-0.47). We make use of the $\delta^{18}O$:$\delta^{13}C$ regression for each individual coral ("lines method") as a reliable proxy to reconstruct temperature at the time of skeletal growth. For this temperature proxy, 95% confidence intervals on the temperature regression are +/- 0.4°C at the mean $\delta^{18}O$ intercept value. The variability required to establish a regression line is apparent both in sampling across the lifetime of the coral (perpendicular to growth axis) as well as within one growth band (parallel to growth axis). Thus, it appears that by analyzing multiple samples within individual corals, a paleotemperature time series may be acquired from the $\delta^{18}O$:$\delta^{13}C$ relationship in bamboo corals. While the relationship between $\delta^{18}O$ and $\delta^{13}C$ in the coral calcite is maintained for the base and branches, the branches exhibit values shifted further away from equilibrium indicating stronger "vital effects" in branch portions of the skeleton.

ACKNOWLEDGEMENTS

We thank the crew and scientific parties of the *R/V Western Flyer,* and *R/V Atlantis* for coral and water sample acquisition. We thank A.C. Neumann, C. Ross and R. Williams for providing Bowditch Seamount and Florida Straits samples. California seamount sampling and geochemical analyses were supported by NOAA West Coast Polar Regions Research Program (NA030AR4300104 to TMH and HJS) and NSF (OCE 0647872 to TMH). Collection of the Warwick Seamount sample was funded by the NOAA Office of Ocean Exploration (NA16RP2637 to TPG), with additional funding by NOAA awards NA05OAR4310017, and NA05OAR4310021. Radiocarbon analyses were performed under the auspices of the U.S. Department of Energy by Lawrence Livermore National Laboratory (contract W-7405-Eng-48) including LLNL IGPP funding (HJS and TPG). We appreciate the technical support of D. Winter, L. Jacobs and staff of LLNL CAMS. DAC and collection of T661 to T669 samples using the *ROV Tiburon* were supported by a grant to MBARI from the David and Lucie Packard Foundation. We thank M. Graziose for the coral photography and B. Gaylord for statistical assistance. We thank R. Thresher and two anonymous reviewers for helpful comments on this manuscript. This is Bodega Marine Laboratory contribution ####.

REFERENCES CITED

Adkins, J.F., McIntyre, K., Schrag, D.P. (2002), The salinity, temperature and $\delta^{18}O$ of the glacial deep ocean. *Science 298*, 1769-1773.

Adkins, J. F., Boyle, E. A., Curry, W., and Lutringer, A. (2003), Stable isotopes in deep-sea corals and a new mechanism for 'vital effects'. *Geochimica et Cosmochimica Acta 67* (6), 1129-1143.

Andrews, A.H., Cailliet, G.M., Kerr, L.A., Coale, K.H., Lundstrom, C., DeVogelaere, A.P. (2005), Investigations of age and growth for three deep-sea corals from the Davidson Seamount off central California. In, *Cold Water Corals and Ecosystems*, Freiwald, A., and Roberts, J.M. (eds), Springer-Verlag, p 1021-1038.

Andrews, A.H., Stone, R.P., Lundstrom, C.C. (2009), Growth rate and age determination of bamboo corals from the northeastern Pacific Ocean using refined 210Pb dating. *Marine Ecological Progress Series 397*, 173-185.

Broecker, W.S.,Olson, E. A. (1961,. Lamont radiocarbon measurements VIII. *Radiocarbon 3*, 176-204.

Cohen, A.L., and McConnaughey, T.A. (2003), Geochemical perspectives on coral mineralization. *Reviews in Mineralogy and Geochemistry* 54 (1), 151-187.

Coplen, T. B. (1993), Report of stable carbon, hydrogen and oxygen isotopic abundances. Reference and Intercomparison Materials for Stable Isotopes of Light Elements. *International Atomic Energy Agency, Technical Document* 825, Vienna, pp.31-38.

Druffel, E.R.M., Griffin, S., Witter, A., Nelson, E., Southon, J., Kashgarian, M., Vogel, J. (1995), *Gerardia*: Bristlecone pine of the deep-sea? *Geochimica et Cosmochimica Acta 59* (23), 5031-5036.

Eltgroth, S.F., Adkins, J.F., Robinson, L, F., Southon, J., Kashgarian, M. (2006), A deep-sea coral record of North Atlantic radiocarbon through the Younger Dryas: Evidence for intermediate water/deepwater reorganization. *Paleoceanography 21*, doi: 10.1029/2005PA001192.

Emiliani, C. Hudson, T.J., Shinn, E.A., George, R.Y. (1978), Oxygen and carbon isotopic growth record in a reef coral from the Florida Keys and a Deep Sea coral from the Blake Plateau. *Science 202* (4368), 627-629.

Epstein, S. and Mayeda, T. (1953), Variation of O^{18} content of waters from natural sources. *Geochimica et Cosmochimica Acta 4*, 213-224.

Guilderson, T.P., Roark, E.B., Flood Page, S.R., Moy, C., Quay, P.D. (2002), Sea water radiocarbon evolution in the Gulf of Alaska: 2002 Observations. *Radiocarbon 48*, 1-15.

Heikoop, J.M., Dunn, J.J., Risk, M.J., Schwarcz, H.P., McConnaughey, T.A., Sandeman, I.M. (2000), Separation of kinetic and metabolic isotope effects in carbon-13 records preserved in reef coral skeletons. *Geochimica et Cosmochimica Acta 64* (6), 975-987.

Heikoop, J.M., Hickmott, D.D., Risk, M.J., Shearer, C.K., Atudorei, V. (2002), Potential climate signals from the deep-sea gorgonian coral *Primnoa resedaeformis*. *Hydrobiologia 471*, 117-124.

Levitus 94: World Ocean Atlas (1994), An atlas of objectively analyzed fields of major ocean parameters at the annual, seasonal, and monthly timescales, http://ingrid.ldeo.columbia.edu/SOURCES/.LEVITUS94/

Myrvold, C.R., Hill, T.M., Spero, H.J. Guilderson, T.P. (2007), Bamboo coral gorgonin: Surface water geochemical records from the organic nodes of a deep water coral. *EOS Transactions, American Geophysical Union* 88 (52) Fall Meeting Supplement.

Noé, S.U. and Dullo, W.-Chr. (2006), Skeletal morphogenesis and growth mode of modern and fossil deep-water isidid gorgonians (Octocorallia) in the West Pacific (New Zealand and Sea of Okhotsk). *Coral Reefs 25*, 303-320.

Noé, S.U., Lembke-Jene, L., and Dullo, W.-Chr. (2008), Varying growth rates in bamboo corals: sclerochronology and radiocarbon dataing of a mid-Holocene deep-water gorgonian skeleton (*Keratoisis* sp.: Octocorallia) from Chatham Rise (New Zealand). *Facies* 54, 141-166.

Ostlund, H.G., and Grall, C., (1987), Transient Tracers in the Ocean North and Tropical Atlantic Tritium and Radiocarbon Report No. 16. University of Miami, 277pp

Roark, E. B., T. P. Guilderson, S. Flood-Page, R. B., Dunbar, B. L. Ingram, S. J. Fallon, and McCulloch, M. (2005), Radiocarbon-based ages and growth rates of bamboo corals from the Gulf of Alaska. *Geophysical Research Letters 32*, doi:10.1029/2004GL021919.

Robinson, L.F., Adkins, J.F., Keigwin, L.D., Southon, J., Fernandez, D.P., Wang, S-L., and Scheirer, D.S. (2005), Radiocarbon variability in the western North Atlantic during the last deglaciation. *Science 310*, 1469-11473.

Sherwood, O.A., Heikoop, J.M., Scott, D.B., Risk, M.J., Guilderson, T.P., and McKinney, R.A. (2005), Stable isotopic composition of deep-sea gorgonian corals

Primnoa spp.: a new archive of surface processes. *Marine Ecology Progress Series 301*, 135-148.

Sherwood, O.A., Edinger, E., Guilderson, T.P., Ghaleb, B., Risk, M., Scott, D.B. (2008). Late Holocene radiocarbon variability in Northwest Atlantic slope waters. *Earth and Planetary Science Letters 275*, 146-153.

Sherwood, O.A., Edinger, E.N. (2009), Ages and growth rates of some deep-sea gorgonian and antipitharian corals of Newfoundland and Labrador. *Canadian Journal of Fisheries and Aquatic Sciences 66* (1), 142-152.

Sikes, E.L., Burgess, S.N., Grandpre, R., Guilderson, T. (2008), Assessing modern deep-water ages in the New Zealand region using deep water corals. *Deep-Sea Research Part I 55*, 38-49.

Sinclair, D.J., Williams, B., Risk. M. (2006), A biological origin for climate signals in corals – Trace element "vital effects" are ubiquitous in Scleractinian coral skeletons. *Geophysical Research Letters 33*, doi: 10.1029/2006GL027183.

Schmidt, G.A., Bigg, G.R., Rohling, E.J. (1999), Global Seawater Oxygen-18 Database. http://data.giss.nasa.gov/o18data/

Smith, J.E, Schwarcz, H.P., Risk, M.J., McConnaughey, T.A. and Keller, N. (2000), Paleotemperatures from deep-sea corals: overcoming 'vital effects'. *Palaios 15*, 25-32.

Stuiver, M., Polach, H.A. (1977), Discussion and reporting of ^{14}C data. *Radiocarbon 19*, 355-363.

Thresher, R., Rintoul, S. R., Koslow, J. A., Weidman, C., Adkins, J., and Proctor, C., (2004), Oceanic evidence of climate change in southern Australia over the last three centuries. *Geophysical Research Letters 31*, doi:10.1029/2003GL018869.

Thresher, R., MacRae, C.M., Wilson, N., Fallon, S. (2009), Feasibility of age determnation of deep-water bamboo corals (Gorgonacea; Isididae) from annual cycles in skeletal composition. *Deep Sea Research Part I:Oceanographic Research Papers 56* (3), 442-449.

Tracey, D.M., Neil, H., Marriott, P., Andrews, A.H., Calliet, G. M., Sanchez, J.A. (2007), Age and growth of two genera of deep sea bamboo corals (family Isididae) in New Zealand waters. *Bulletin of Marine Science 81* (3), 393-408.

Urey H. C. (1947), The thermodynamic properties of isotopic substances. *Journal of Chemical Physics*, 562–581.

TABLES

CORAL ID	Longitude W	Latitude N	Depth (m)	Basal Diameter (cm)	Location	Collection Method
ALV3803 #3	-132.73	48.05	720	1.8	Warwick Seamount, GoA	Submersible
BB (Bodega)	-123.50	38.50	250	2.0	offshore Bodega Head, CA	Fishing trawl
T1104 A7	-122.04	36.74	870	2.5	Monterey Canyon, CA	Submersible
T661 A9	-121.08	34.05	792	2.0	Rodriguez Seamount, CA	Submersible
T664 A1	-120.88	33.15	2055	3.5	San Juan Seamount, CA	Submersible
T664 A17	-120.91	33.13	1295	3.0	San Juan Seamount, CA	Submersible
T669 A1	-121.48	32.64	2043	7.5	San Marcos Seamount, CA	Submersible
T668 A13	-120.05	31.91	2136	5.0	Little Joe Seamount, CA	Submersible
BE 1	-64.53	32.74	1395	0.7	Bowditch Seamount, NW Atlantic	Dredge
FL-17-XI-05-1-11	-79.839	26.09	940	1.5	Florida Straights, NW Atlantic	Submersible

Table 1. Coral samples utilized for the $\delta^{18}O$:$\delta^{13}C$ linear regression.

Coral ID	Average band width (um)	SE	SD
T664 A1 base	77	10	34
T664 A1 branch	126	15	33
T664 A17 base	21	2	11
T668 A13 base	61	14	45
T668 A13 branch	14	2	9
T669 A1 base	61	15	52
T669 A1 branch	22	2	12

Table 2. Coral growth band measurements from the outer 1 mm on base and branch thin sections, standard error and standard deviation.

ID	Type	Distance from edge	Water depth	$D^{14}C$ (‰)	^{14}C Age	Radial extension rate - (μm/^{14}C year)	Radial extension rate - band width (μm/year)
BB	coral calcite	0-1 mm	250m	-220.3 +/- 3.1	2000 +/- 35		
BE 1	coral calcite	0-1mm	1395m	-74.8 +/- 3.8	570 +/- 35		
T664 A1 base	coral calcite	1-2 mm	2055m	-257 +/-2.6	2385 +/- 30	38-89	43-111
T664 A1 base	coral calcite	9-10 mm	2055m	-270.6 +/- 2.7	2535 +/- 30		
T664 A17 base	coral calcite	0-1 mm	1295m	-221.3 +/- 3.0	2125 +/- 35	34-58	10-32
T664 A17 base	coral calcite	11-12 mm	1295m	-256.6 +/- 2.4	2380 +/- 30		
T668 A13 base	coral calcite	0-1.5 mm	2136m	-249.7 +/-3.6	2255 +/- 40	42-66	16-106
T668 A13 base	coral calcite	18.5-19.5 mm	2136m	-281.6 +/-3.0	2605 +/- 35		
T669 A1 base	coral calcite	0-1 mm	2043m	-252.3 +/-2.9	2335 +/- 35	80-128	9-113
T669 A1 base	coral calcite	34.5-35.5 mm	2043m	-284.3 +/-3.9	2685 +/- 45		
T669 A1 branch	coral calcite	0-1 mm	2043m	-258.8 +/- 3.5	2405 +/- 40	18-28	10-34
T669 A1 branch	coral calcite	7-8 mm	2043m	-287.8 +/- 2.4	2725 +/- 30		
T662 N1	seawater DIC		1842m	-268.9 +/- 3.4	2515 +/- 40		
T664 N2	seawater DIC		1954m	-229.4 +/- 2.7	2040 +/-30		
T664 N2 (dupl)	seawater DIC		1954m	-231.0 +/- 2.1	2055 +/- 25		
T669 N1	seawater DIC		2043m	-242.2 +/- 2.6	2175 +/-30		
T669 N1 (dupl)	seawater DIC		2043m	-234.3 +/- 4.0	2090 +/-45		
T668 N1	seawater DIC		2136m	-230.9 +/- 3.6	2110 +/- 40		

Table 3. Radiocarbon data for corals from California margin and Bowditch Seamount, NW Atlantic. Seawater samples listed were taken near California coral sampling sites. Distance from edge denotes location where radiocarbon sample was acquired. Duplicates were analyzed for two of the seawater DIC samples. We then compare radial extension rates based upon ^{14}C analyses (uncalibrated ages) and band width measurements from Table 2.

555

556 Table 4. Data for the $\delta^{18}O$:$\delta^{13}C$ linear regression (Figure 4) in this study. These data are not corrected for local $\delta^{18}O_w$ and $\delta^{13}C_{DIC}$ values.

557

Coral ID	$\delta^{13}C$	$\delta^{18}O$
ALV3803 #3	-3.50	0.94
	-3.31	0.88
	-3.27	0.85
	-3.40	0.98
	-3.32	0.68
	-3.45	0.52
	-3.75	0.90
	-3.74	0.74
	-3.45	0.97
	-3.59	0.85
	-3.38	0.95
	-3.34	1.03
	-3.50	1.02
	-3.08	1.03
	-3.16	0.93
	-3.21	1.00
	-3.48	0.95
	-3.69	0.77
	-3.93	0.72
	-4.23	0.72
	-4.45	0.53
	-4.30	0.38
BB (Bodega)	-4.36	0.30
	-3.87	0.38
	-3.63	0.68
	-3.63	0.64
	-3.18	0.71
	-2.99	0.82
	-2.33	0.82
	-2.62	0.76
	-2.87	0.80
	-2.87	0.80
	-3.10	0.72
	-2.45	0.74
	-1.94	0.87
	-1.81	1.06
	-1.81	1.02
	-1.88	1.05
	-2.36	0.85
	-2.12	0.91
	-1.98	0.91
	-2.33	0.94
	-1.78	1.19
	-1.47	1.29

BB (Bodega)	-1.71	1.25
(cont)	-1.72	1.29
	-1.76	1.19
	-1.71	1.16
	-2.34	1.09
	-2.50	0.97
	-1.49	1.12
	-1.40	1.20
	-1.28	1.36
	-1.52	1.13
	-1.39	1.21
	-1.11	1.31
	-1.28	1.21
	-2.04	1.05
	-1.33	1.26
	-1.46	1.30
	-2.13	1.01
	-2.16	0.96
	-2.13	1.09
	-1.96	1.04
	-2.12	0.96
	-2.09	0.96
	-1.84	1.02
	-1.53	1.20
	-1.26	1.28
	-1.34	1.18
	-1.31	1.24
	-1.41	1.20
	-1.83	1.15
	-2.02	1.02
	-1.53	1.12
	-1.70	1.24
	-3.17	1.61
	-1.60	1.20
	-1.36	1.30
	-1.52	1.25
	-1.42	1.30
	-1.77	1.22
	-1.39	1.23
	-1.50	1.16
	-1.61	1.19
	-1.66	1.25
	-2.05	1.15
	-2.27	1.13
	-2.50	1.00
	-2.40	1.08

BB (Bodega)	-2.30	1.08
(cont)	-1.97	1.12
	-2.10	1.15
T1104 A7	-2.64	0.92
	-3.59	0.75
	-2.90	0.94
	-3.99	0.30
	-3.51	0.49
	-2.29	0.75
	-3.20	0.60
	-4.47	0.07
	-1.56	1.24
	-2.73	1.05
	-3.29	0.86
	-3.55	0.67
T661 A9	-4.12	0.48
	-4.38	0.61
	-4.86	0.40
	-5.18	0.41
	-4.64	0.30
	-4.81	0.08
	-5.23	0.09
	-3.45	0.91
	-3.43	0.70
	-3.30	0.73
	-3.65	0.69
	-3.93	0.58
T664 A1	-1.64	2.37
	-1.16	2.56
	-1.32	2.41
	-1.23	2.44
	-0.96	2.63
	-0.95	2.49
	-1.08	2.45
	-1.40	2.18
	-1.24	2.32
	-1.55	2.21
	-2.50	1.81
	-3.38	1.85
T664 A1	-4.27	1.12
branch	-3.61	1.42
	-3.57	1.39

T664 A1	-3.88	1.27
branch	-3.81	1.39
(cont.)	-3.45	1.60
	-3.78	1.37
	-3.85	1.43
	-3.22	1.55
	-5.68	0.95
	-5.31	0.80
	-5.37	0.84
	-5.24	0.80
	-6.03	0.50
	-5.17	0.79
	-5.46	0.61
T664 A17	-2.96	1.62
	-3.54	1.36
	-3.19	1.41
	-1.85	1.79
	-1.56	1.85
	-2.22	1.56
	-2.02	1.82
	-2.03	1.80
	-2.00	1.82
	-2.31	1.69
	-1.82	1.80
	-2.17	1.69
	-2.31	1.59
	-5.00	0.84
T669 A1	-2.45	1.87
	-2.38	1.91
	-2.16	1.92
	-1.96	1.93
	-2.09	1.97
	-2.11	1.83
	-1.98	1.87
	-2.48	1.69
	-2.52	1.69
	-2.26	1.73
	-1.93	1.83
	-1.97	1.81
	-1.90	1.92
	-2.43	1.67
	-1.67	2.14
	-1.89	2.12

T669 A1	-1.86	2.09
(cont.)	-1.39	2.16
	-1.42	2.17
	-1.66	2.17
	-1.60	2.17
	-1.30	2.26
	-1.34	2.08
	-1.39	2.12
	-1.63	2.11
	-1.55	2.28
	-2.35	1.85
	-3.26	1.56
	-4.55	1.36
T669 A1	-5.31	0.80
branch	-5.37	0.84
	-5.24	0.80
	-6.03	0.50
	-5.17	0.79
	-5.46	0.61
T668 A13	-1.26	2.25
	-1.58	2.02
	-1.30	2.29
	-1.74	2.02
	-1.52	1.85
	-1.21	2.28
	-2.00	2.05
	-2.04	1.87
	-2.48	1.63
	-2.00	1.86
	-1.79	1.91
	-2.35	1.94
	-1.44	2.17
	-1.05	2.47
	-1.39	2.12
	-1.55	1.93
	-1.87	2.17
	-2.07	1.97
	-3.13	1.66
T668 A13	-3.78	1.37
branch	-3.85	1.43
	-3.22	1.55
	-5.68	0.95

BE 1	0.59	2.07
	0.80	1.93
	0.85	1.85
	0.74	1.79
	0.40	1.66
	0.57	1.43
	0.96	2.16
	0.62	1.77
	0.95	2.10
	0.84	2.03
	1.10	1.89
	1.86	2.18
FL-17-XI-05-1-11	1.29	1.33
	1.51	1.27
	1.14	1.65
	0.82	1.24
	1.08	0.97
	1.30	1.05
	0.68	0.81

Coral	Eqn	N	R^2	R	P value
T664 A1	y=0.47x+3.17	11	0.84	0.92	0.001
T668 A13	y=0.40x+2.89	18	0.63	0.79	0.001
T669 A1	y=0.38x+2.87	28	0.79	0.89	0.001
T664 A17	y=0.25x+2.41	14	0.83	0.91	0.001
BB	y=0.30x+1.81	69	0.82	0.91	0.001
3803-3	y=0.35x+2.03	22	0.49	0.70	0.001
BE 1	y=0.37x+1.51	12	0.38	0.62	0.1
FL-17-XI-05-1-11	y=0.18x+0.81	11	0.07	0.26	n/a
T661 A9	y=0.32x+1.99	12	0.75	0.87	0.001
T1104 A7	y=0.36x+2.02	12	0.76	0.87	0.001

Table 5. Regression statistics for each coral in Figure 4 (base samples only). FL-17-XI-05-1-11 is excluded from Table 6 and Figure 6 due to poor statistical significance. BB is excluded from Table 6 and Figure 6 because it was acquired via fishing trawl and exact depth (and temperature) is unknown.

ID	Intercept	Temperature (°C)
T664 A1	3.17	2.0
T668 A13	2.89	2.0
T669 A1	2.87	2.0
T664 A17	2.24	3.5
3803-3	2.03	3.5
T1104 A7	2.01	4.5
T661 A9	1.99	4.5
BE 1	1.51	5.0

Table 6. Intercepts for regression of $\delta^{18}O$ vs $\delta^{13}C$, where $\delta^{13}C = 0$; temperatures from Levitus dataset.

FIGURE CAPTIONS

Figure 1. Bamboo coral (BB) collected in fisherman's dredge in the Bodega Bay region, showing branching morphology and presence of calcite internodes and gorgonin nodes. Total coral length 20cm.

Figure 2. Map of study area with coral sampling locations noted.

Figure 3. $\delta^{18}O$ (blue triangles) and $\delta^{13}C$ (red squares) of coral calcite plotted versus distance from the edge of the coral for coral BB. Lowest values are found near the central (core) region of the coral. Photomicrograph shows coral banding and micromilling tracks from sampling (center of coral is identified by the hole on right side of micrograph). These data are included in the $\delta^{18}O$:$\delta^{13}C$ regression shown in Figure 4, but the most depleted points from the center are excluded.

Figure 4. $\delta^{18}O$ and $\delta^{13}C$ values for the base sections of the 10 corals studied here: T664 A1 (blue diamonds), T668 A13 (red squares), T669 A1 (purple circles), T664 A17 (black x), ALV3803-3 Warwick Seamount (black hollow boxes), BB (grey *), T1104 A7 (blue hollow circles), T661 A9 (green hollow diamonds), FL-17-XI-05-1-11 Florida Straights (green triangles) and BE Bowditch Seamount (grey squares). Data are corrected for $\delta^{18}O_w$ and $\delta^{13}C_{DIC}$ using values listed in results section.

Figure 5. Carbon and oxygen stable isotopic values for the base (filled symbols) and branch (empty symbols) sections of three of the corals studied here. Symbols are the same as in Figure 5: T664 A1 (blue diamonds), T668 A13 (red squares), T669 A1 (purple circles). Note x axis has changed from Figure 5. Data are corrected for local $\delta^{18}O_w$ and $\delta^{13}C_{DIC}$. The consistent relationship between $\delta^{13}C$ and $\delta^{18}O$ is maintained through base and branch, but larger fractionation from equilibrium is exhibited by branch specimens.

Figure 6. The $\delta^{18}O$ value at $\delta^{13}C$=O intercept for the corals studied here (base only), plotted versus temperature (from Levitus dataset). Blue squares represent 8 bamboo corals investigated here. Grey squares represent data from 18 aragonitic deep sea coral species that are closest in temperature range with our dataset (additional data available from Smith et al., 2000). Both datasets were corrected for local $\delta^{18}O_w$ and $\delta^{13}C_{DIC}$. 95% confidence intervals are indicated by dashed lines around each regression.

Figure 7. Geochemistry of calcite collected from a single growth band (10 mm from margin) in coral BB. Sample resolution is 2-4 mm. Data are corrected for local $\delta^{18}O_w$ and $\delta^{13}C_{DIC}$.

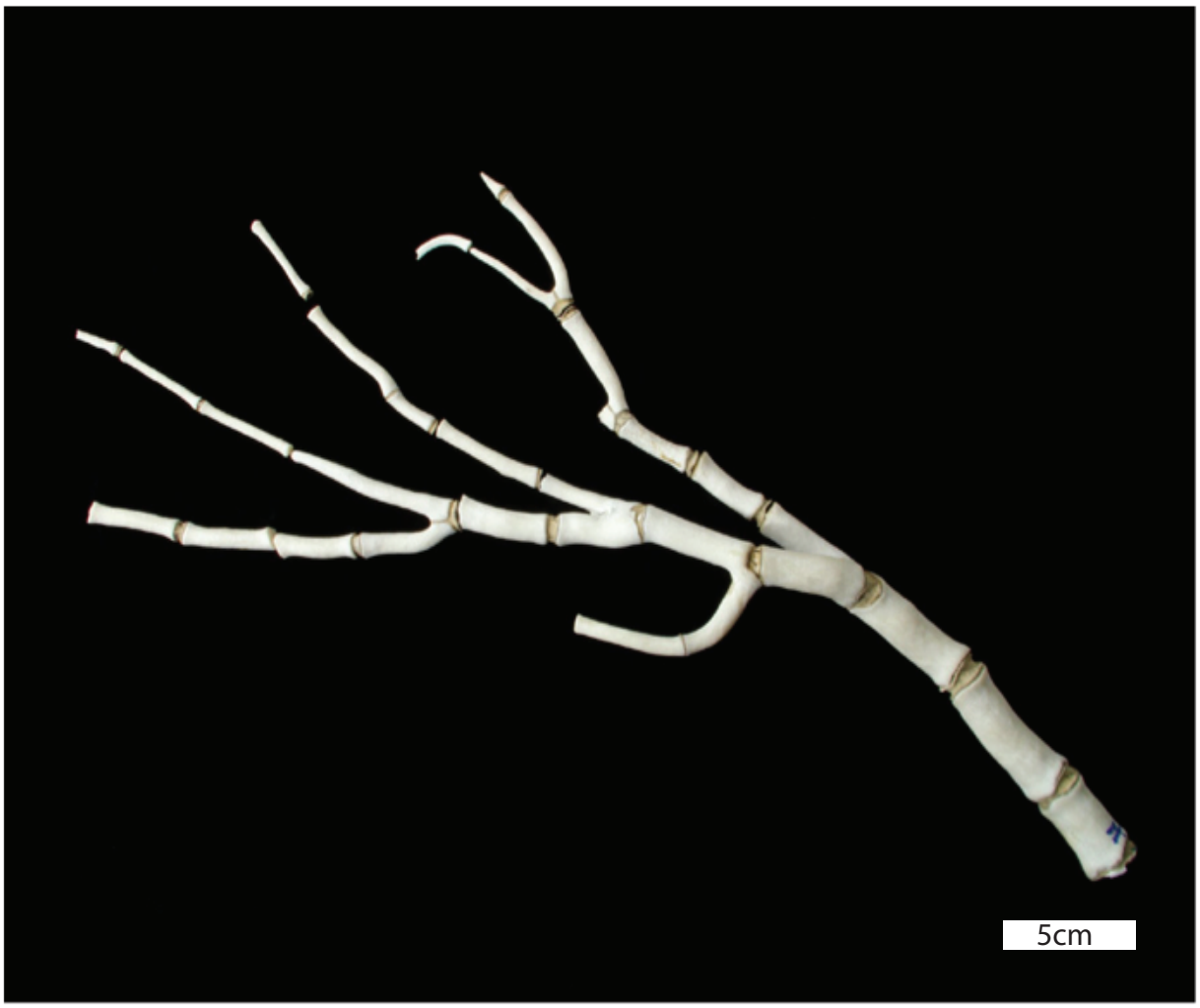

Figure 1.

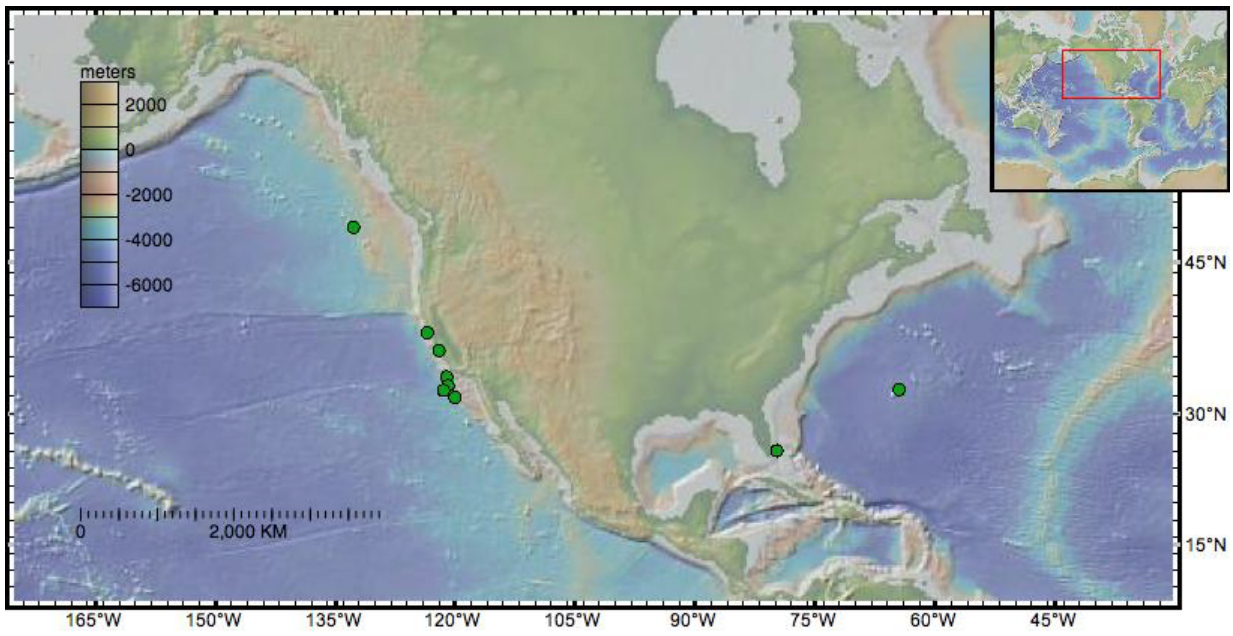
meters
2000
0
-2000
-4000
-6000
0
2,000 KM
45°N
30°N
15°N
165°W
150°W
135°W
120°W
105°W
90°W
75°W
60°W
45°W

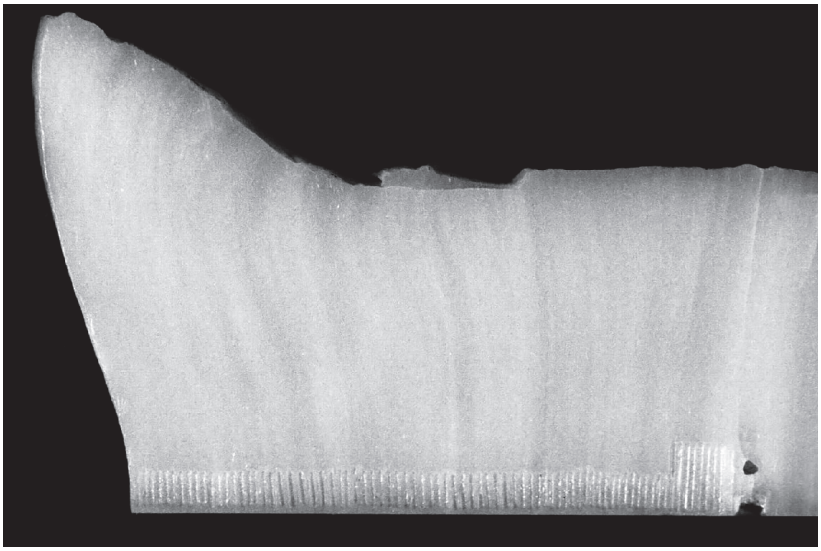

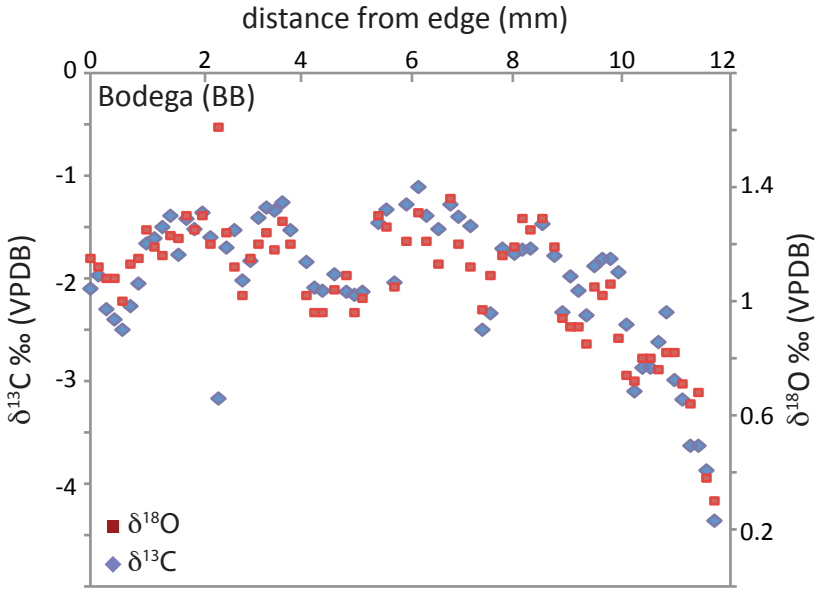
distance from edge (mm)
0
2
4
6
8
10
12
Bodega (BB)
0
-1
-2
-3
-4
1.4
1
0.6
0.2
δ13C ‰ (VPDB)
δ18O ‰ (VPDB)
δ18O
δ13C

Figure 3.

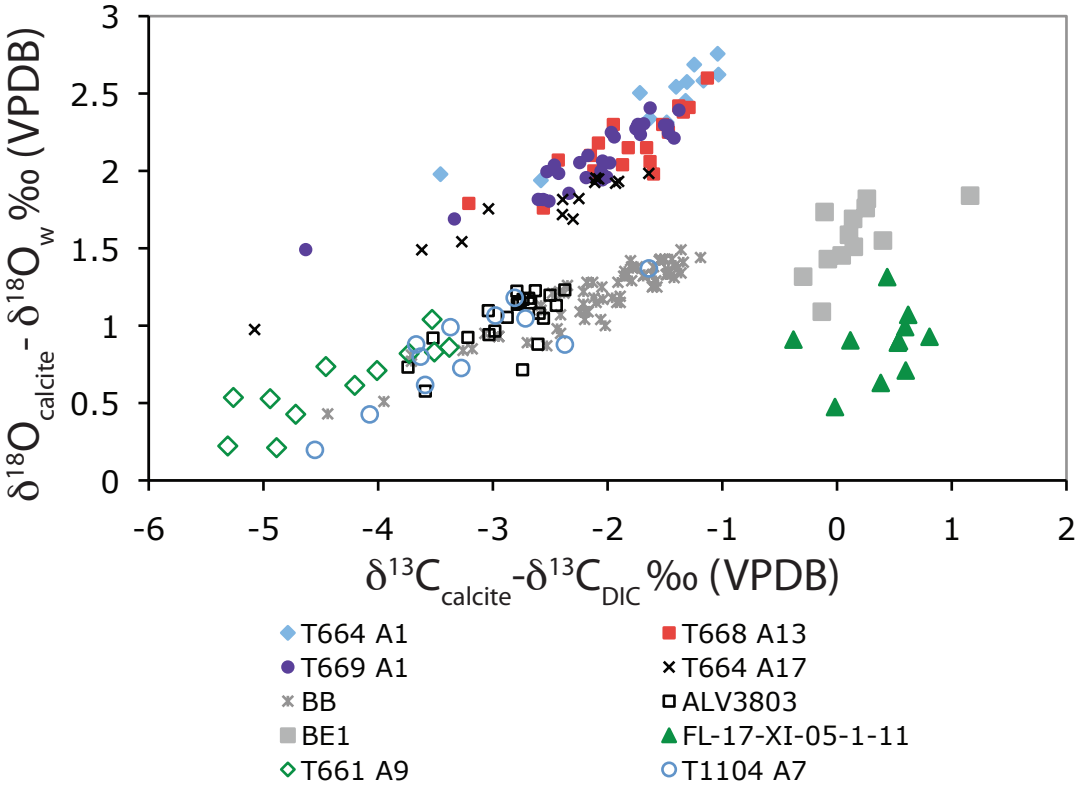
3
2.5
2
1.5
1
0.5
0
-6
-5
-4
-3
-2
-1
0
1
2
δ18Ocalcite - δ18Ow ‰ (VPDB)
δ13Ccalcite -δ13CDIC ‰ (VPDB)
T664 A1
T668 A13
T669 A1
T664 A17
BB
ALV3803
BE1
FL-17-XI-05-1-11
T661 A9
T1104 A7

Figure 4.

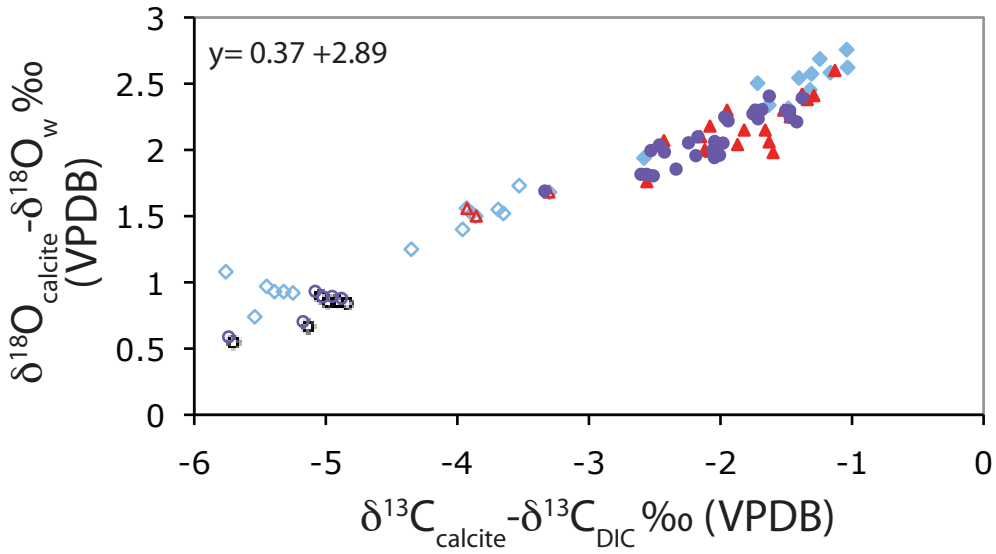
y= 0.37 +2.89
3
2.5
2
1.5
1
0.5
0
-6
-5
-4
-3
-2
-1
0
δ18Ocalcite-δ18Ow ‰ (VPDB)
δ13Ccalcite-δ13CDIC ‰ (VPDB)

Figure 5.

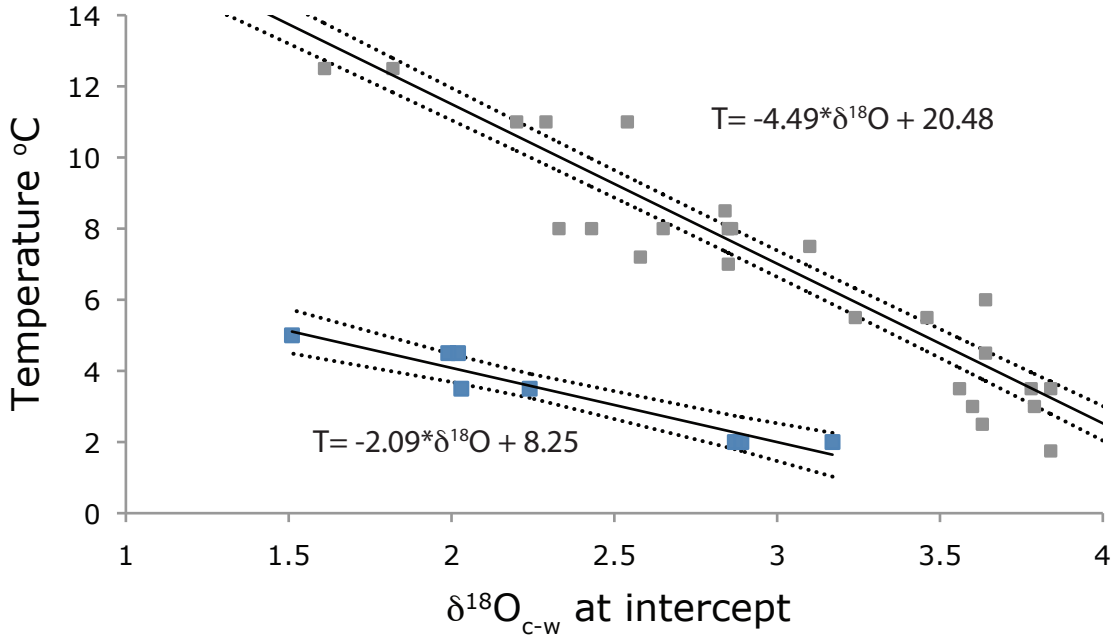
Temperature °C
14
12
10
8
6
4
2
0
1
1.5
2
2.5
3
3.5
4
T= -4.49*δ18O + 20.48
T= -2.09*δ18O + 8.25
δ18Oc-w at intercept

Figure 6.

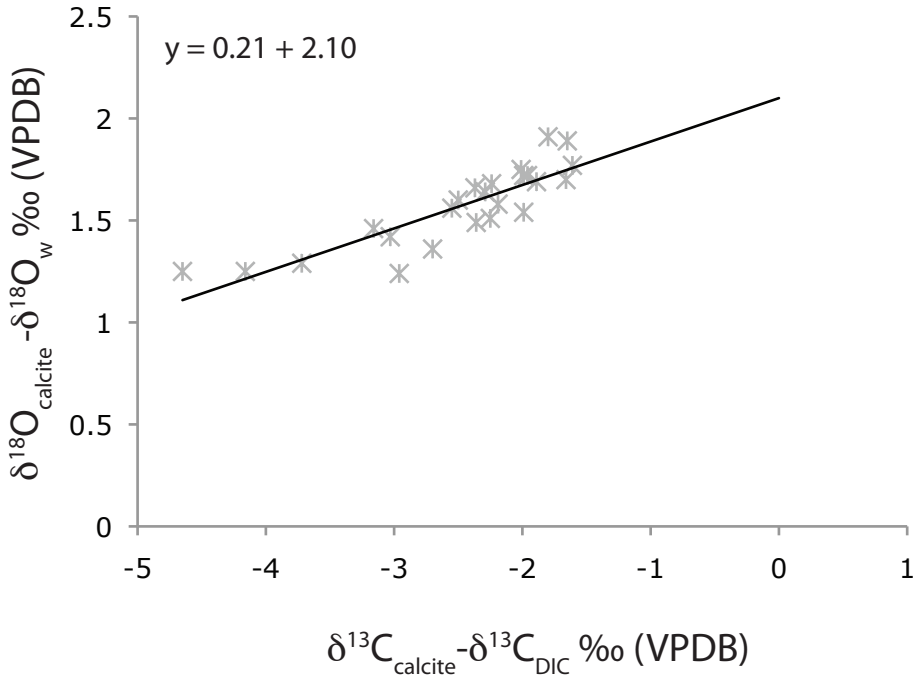
y = 0.21 + 2.10
2.5
2
1.5
1
0.5
0
-5
-4
-3
-2
-1
0
1
δ18Ocalcite-δ18Ow ‰ (VPDB)
δ13Ccalcite-δ13CDIC ‰ (VPDB)

Figure 7.